Rope mesh as a seismic reinforcement for two-storey adobe buildings

Tarque Nicola[1*], Blondet Marcial[1], Vargas-Neumann Julio[1] and Yallico-Luque Ramiro[1]

[1] GERDIS Research Group, Civil Engineering Division, Pontificia Universidad Católica del Perú, Av. Universitaria 1801, Lima, Peru

*Corresponding author: sntarque@pucp.edu.pe

ABSTRACT

Throughout the world, millions of people are at risk because they live in unreinforced earthen dwellings, which have consistently shown extremely poor structural behaviour during earthquakes. Every single earthquake occurring in these areas has caused unacceptable loss of life, injuries, and property damage. Earthquakes are recurrent and construction damage is cumulative. It is urgent, therefore, to devise low-cost, easy-to-implement seismic reinforcement systems and to make them available to the actual dwellers.

A group of researchers at the *Pontificia Universidad Católica del Perú (PUCP)* has been working towards that goal, especially on improving the seismic capacity of one-storey adobe dwellings. They have proposed construction methodologies for a seismic reinforcement system consisting of a mesh of nylon ropes that confines all earthen walls. This reinforcement system would control the wall displacements and prevent the overturning of wall portions that may occur due to seismic shaking.

To validate the effectiveness of the nylon rope mesh reinforcement on two-storey adobe dwellings, shaking table tests were conducted on unreinforced and half-scale reinforced adobe models, simulating the actions of slight, moderate and strong seismic ground shaking. These models were designed to include the main construction features of typical adobe dwellings in the Peruvian Andes. The results of the experimental tests showed that the rope mesh reinforcement system was able to preserve the structural stability of the tested reduced-scale adobe models under strong motions, thus preventing collapse. It is expected that the proposed reinforced system would also improve the seismic performance of one and two-storey adobe dwellings, reducing in this way their inherent high seismic risk.

Keywords: adobe masonry, strengthening, shaking table, seismic capacity, experimental dynamic tests, rope mesh reinforcement

1. Introduction

Adobe is a Spanish word derived from the Arabic *atob*, which means sun-dried brick. Adobe is one of the oldest and most widely used natural building materials because the soil for construction is easily available (Houben and Guillaud 1994, Correia 2016). Adobe walls are composed of bricks joined by a mortar made from the same soil as the adobe blocks. Furthermore, adobe masonry has good thermal properties because the earthen walls absorb heat during the day and radiate heat at night, keeping rooms comfortable for living in hot climates such as in Latin America, the Middle East or Africa (Avrami et al. 2008, Blondet et al. 2011).

The use of sun-dried blocks dates back to around 8000 BC. Archaeological evidence shows entire cities built of raw earth, such as Jericho, the oldest city in history; Çatal Hüyük in Turkey; Harappa and Mohenjo-Daro in Pakistan; Akhlet-Aton in Egypt; Chan-Chan in Peru; Babylon in Iraq; Duheros near Cordoba in Spain and Khirokitia in Cyprus (Easton 2007). Earthen housing is a traditional housing solution in many developing countries because soil is abundant and cheap. However, most adobe houses are built without technical assistance and therefore with poor construction quality, resulting in high seismic vulnerability (Sumerente et al. 2020, Tarque et al. 2012). In addition, contemporary adobe houses tend to imitate the architectural features of clay masonry buildings: several stories, thin walls, large openings, and irregular configurations, see Figure 1a. As a result, earthquakes around the world have caused tragic human losses, extensive property damage and the destruction of invaluable historical monuments (Berge 2009, Blondet et al. 2017, Brando et al. 2019, Costa et al. 2014).

The collapse of unreinforced earthen constructions is triggered by the progressive formation of cracks in the walls. The most common types are x-shaped cracks due to shear, and vertical corner cracks (Figure 1b). In addition, vertical corner cracks may be followed by overturning of exterior walls. According to a damage survey conducted after an earthquake in Peru in 2007, the most common failure observed in unreinforced adobe buildings was the overturning of the façade and their collapse onto the street (Tarque et al. 2021). This was because the strength of the wall at the intersection between the façade and the other house walls was too low to withstand the movement of the earthquake. In addition, the study of the damage has shown that the extent of damage was directly related to whether the roof's wooden joists were connected -or not- to the top of the façade . If the façade had supported the roof joists, the wall's collapse would have unbalanced them, causing the roof to collapse as well. On the other hand, the roof would not have collapsed if the walls perpendicular to the façade had supported the joists (Figure 1b).

a) 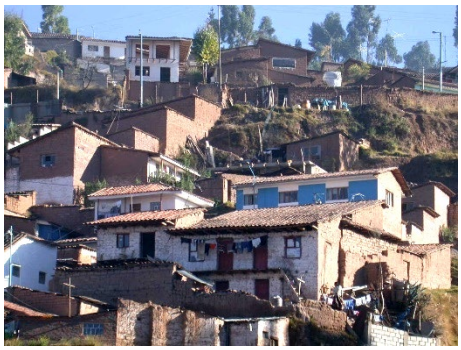 b) 

Figure 1. (a) Contemporary adobe houses in Cusco, Peru; (b) Out-of-plane failure of adobe walls during the Pisco (Peru) earthquake of 2007.

The severe seismic damage on adobe buildings is mainly due to the lack of appropriate structural reinforcement of their walls (Dowling 2004, Ismail and Khattak 2016, Webster and Tolles 1994). Researchers from many universities have therefore been working since the 1970s to find cost-effective and simple ways to provide seismic safety for earthen buildings. Reinforcement proposals and repair systems included internal or external wall reinforcements. For example, an internal cane mesh was created by anchoring vertical cane rods to a concrete foundation and tying them to horizontal layers of crushed canes placed within the mortar every few adobe rows (Fig. 2a). The vertical cane rods are then tied to a wooden crown beam placed at the top of the walls. A detail of this reinforcement is included in the Peruvian Code (NTE E080 2020, Figure 2b).

a)  b) 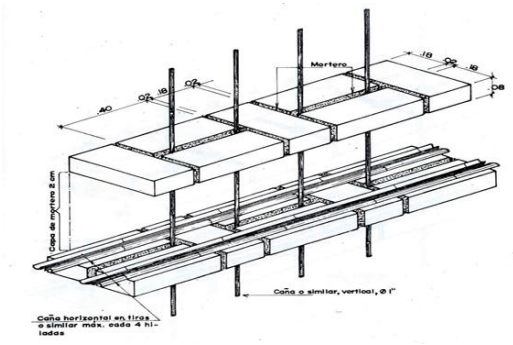

Figure 2. Internal cane mesh strengthening system. a) Example of application, b) mesh layout (modified from NTE E080 2020)

Seismic simulation tests of full-scale one-storey adobe models have shown that the cane mesh reinforcement increases the out-of-plane flexural and in-plane shear strength of adobe walls. The limitation of this strengthening system is that cane is not available in all seismic regions. Moreover, in areas where cane is produced, it is practically impossible to obtain the required quantity for a massive construction or

reconstruction program. The use of cane as seismic reinforcement also requires more effort on the part of the builders; therefore, the inhabitants prefer to build without reinforcement.

The use of mortar to repair cracks in adobe walls is classified as an internal repairing system. Blondet et al. (2013), Figuereido et al. (2013) and Muller et al. (2016) studied grout injection to repair earthquake-damaged earthen buildings. The idea was to use fluid mortars to fill cracks and discontinuities. Vargas et al. (2008) validated the efficiency of fluid mortars through diagonal compression tests on small adobe walls. Although the grout was able to restore the initial tensile strength of the material, the failure of the masonry did not improve. Therefore, the use of external strengthening as supplementary reinforcement was recommended. Furthermore, Silva et al. (2009, 2012) used unstabilized mud grouts for application in earthen constructions. The most important finding was that the higher the clay content, the higher the flexural and the compressive strength, but an excessive clay content is not beneficial for the grout rheological behaviour (Parisi et al. 2021).

Regarding the use of external strengthening systems, different alternatives were successfully applied on adobe single storey adobe models. For example, Torrealva et al. (2006) validated (through dynamic tests) the cane-rope grid system's effectiveness. This grid is composed of vertical canes placed on the external faces of all walls, tied together with horizontal ropes. During the dynamic tests on adobe models, the cane-rope grid system provided confinement to the adobe structure and avoided collapse during shaking. In addition, Blondet et al. (2005) investigated the use of diverse industrial materials to improve the adobe masonry's seismic performance. Here a series of cyclic tests were performed on full-scale I shaped walls (Figure 3). Three baseline walls were studied: an unreinforced wall, a wall reinforced with an internal cane mesh, and an external wire mesh covered with cement mortar. In addition, the following alternative reinforcement solutions were also investigated: vertical PVC tubes anchored to the foundation and to the crown beam, tied with simple plastic mesh placed inside the mortar; single steel reinforcement bars at the corners, anchored to the foundation and to the concrete crown beam; and geosynthetic mesh externally fixed to both sides of the wall. The geosynthetic mesh offered the best improvement in the response, since it increased the displacement ductility and prevented global instability . This conclusion was further verified with static and dynamic tests performed by Laucotre et al. (2007), Bossio et al. (2013), and Figuereido et al. (2013).

a)  b) 

Figure 3. Cyclin in-plane tests on adobe walls strengthened with: a) welded wire mesh and b) geosynthetic mesh (Blondet et al. 2005)

Zegarra et al. (1997, 2001) conducted experimental tests on adobe modules reinforced with vertical and horizontal strips of welded wire mesh covered with cement mortar, simulating beams and columns in the building corners. The wire meshes were connected through the wall thickness with wire. Experimental tests showed that although this strengthening system works well for moderate earthquakes, the adobe models failed in a brittle manner under severe ground motions. Reyes et al. (2019) also performed dynamic tests but on 1:5 scaled two-storey adobe modules. One of the samples was reinforced with wire mesh welded at the corners of the walls. Again, the behaviour for strong shakes was not adequate because there was a separation of the reinforced wall areas from the unreinforced wall ones. Also, reinforced concrete confinement elements were studied by some authors (San Bartolomé et al. 2009, Khan al. 2021) to reinforce the adobe masonry. Although RC elements improved the lateral strength of the structures, the increment in displacement ductility was limited.

The use of meshes made of natural fibres as seismic strengthening of adobe masonry is advantageous due to the good physical and mechanical properties of the fibres, and especially due to the low carbon footprint of the materials. In this sense, Parisi et al. (2013, 2015) performed eight diagonal compression tests on adobe masonry samples strengthened with a bidirectional hemp fibre placed around the walls. The mesh allowed smeared cracking to occur within the masonry samples, controlling the thickness of cracking and improving the displacement ductility of the adobe walls, without increasing the initial stiffness compared to the unreinforced samples. However, as the researchers say, the variability of the mechanical properties and durability of the fibres needs to be further investigated.

Recently, the PUCP's GERDIS research group has developed and proposed an innovative reinforcement system conceived to prevent the overturning of wall portions during earthquakes. The proposed reinforcement system, consisting of enveloping all the walls with a mesh made of synthetic ropes that

completely envelopes all the walls, was successfully validated at the PUCP's Structures Laboratory (Blondet et al. 2016, 2019). In a first experimental project, two one-storey adobe models (full-scaled) were built, reinforced with nylon string meshes and tested at the unidirectional shaking table. The first one-storey model (Blondet et al. 2016) was first shaken to induce representative seismic damage. Then, the model was repaired and reinforced with a mesh made of 1/4" nylon ropes. All ropes were tensioned using metal turnbuckles. The meshes on both faces of each wall were joined together by 1/8" nylon ropes, which crossed the walls through the mortar joints at selected places. The model was tested again on the shaking table with a sequence of movements of increasing intensity (0.30 g, 0.71 g, 1.08 g and 1.53 g horizontal base acceleration). The seismic response was excellent because, even during the strongest shaking, the mesh reinforcement maintained the structural connection between roof and walls, thus controlling the excessive displacements of the walls (Figure 4a). The second model was similar to the first but reinforced with a mesh made of 5/32" hand-tied nylon ropes, and subjected to just one strong motion at the shaking table (Figure 4b). Again, the results validated the efficiency of the nylon ropes in preventing the wall from collapsing. The reinforcement ratio was determined through the evaluation of typical failure mechanisms, as proposed by Blondet et al. (2019). Here, a single line of 5/32” rope was placed every two horizontal adobe rows from the base up to the window lower part; then, two lines of 5/32” ropes were placed every adobe row up to the roof. The spacing of the vertical ropes was equal to the length of one adobe brick (Figure 4b).

a)  b) 

Figure 4. Full-scale one-storey adobe models after shaking table tests. (a) First model (b) second model

Although this reinforcement system has been considered suitable for one-storey buildings, it does not solve the question of whether the same reinforcement may also be suitable for the seismic protection of two-storey adobe buildings. In the Andean region, it is common to find two-storey earthen houses. For example, Figure 5 shows views of two cities placed in the South Central of Peru, where many two-storey houses can be seen.

a)  b) 

Figure 5. A view of the cities of (a) Huancayo and (b) Cusco.

In a second experimental project, the PUCP researchers decided to assess whether the proposed rope mesh reinforcement would also be effective in providing seismic safety to multi-storey earthen constructions. This article shows the results of a project consisting of four experimental dynamic tests performed on reduced scale two-storey adobe models, two of them without any reinforcement, and the other two with the proposed rope mesh.

Weight limitations of the test specimens of the PUCP seismic simulator do not allow for dynamic testing of full-scale models of two-storey adobe buildings. Also, the platform size prevents the construction of full-scale typical buildings. It was decided, therefore, to test reduced-scale specimens. The largest two-storey adobe structure that could be tested under realistic seismic motions with the equipment available, would be a half-scale one-room, two-storey building. It is clear that such buildings do not exist in the field. Furthermore, the structural response of adobe masonry under seismic excitations is highly nonlinear, as mortar cracking occurs at very low tensile stresses, and therefore any linear scaling theory ceases to be valid. Nevertheless, a scaling process was used to design the test models and to generate the shaking table command signal, in order to comply with the equipment restrictions and to retain the main features of typical adobe construction in the Peruvian Andes. No attempt was made, therefore, to correlate the dynamic response of the reduced scale test specimens with that of any specific full-scale prototype structures.

The main objective of the project was thus to determine the viability of the proposed rope mesh reinforcement system to protect two-storey adobe structures. Two main aspects were considered important: 1) the capability and effectiveness of the rope reinforcement to prevent partial (and total) collapse of the adobe walls, and 2) the practical procedure required to place the reinforcement ropes in such a way that they completely enveloped all the walls.

2. Typology of two-storey adobe dwellings in Peru

A typical adobe house was selected to have a preliminary notion of the architectural characteristics of the models to be tested on the shaking table. Most two-storey adobe houses in Peru have simple rectangular, L-shaped or C-shaped plan configurations. For example, Figure 6 shows an L-shaped adobe house and its plan view configuration. The first level is used as a social area in which the living room and dining room can be independent. There are also rooms that communicate through a central or lateral corridor (Carazas, 2001). The second level maintains the same dimensions as the first level and is intended mainly for bedrooms. The roof can be gabled or with a single slope. The first level has an average height of 2.50 m and the second level of 2.30 to 2.40 m. At the highest point of the roof, the house can reach a height of approximately 7 m.

a)  b) 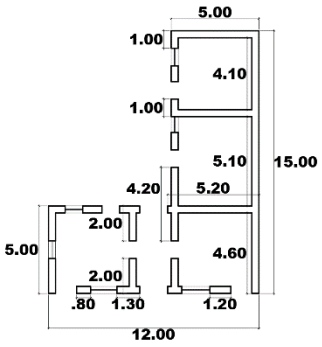

Figure 6. a) "L" shaped two-storey adobe house, b) plan distribution of 1st and 2nd stories.

Most adobe houses are built with traditional materials such as adobe blocks, eucalyptus rods, corrugated clay tile, gypsum, stone and straw, without any additional reinforcement. The depth of the stone foundations can vary between 0.50 to 0.80 m, depending on the thickness of the wall. The foundation stones are joined with mud mortar, with the larger stones at the bottom of the wall. The stone plinth has the same thickness as the wall and is made of medium-sized stones, mostly flat, also joined with mud mortar. The beams that support the wooden floors are made of round eucalyptus rods (0.20 m diameter). These beams are installed directly on the adobe walls, with an approximate separation of 0.80 m. The doors and windows are made of medium-quality wood. The dimensions of the windows vary between 1.00 to 1.50 m and the doors are between 1.90 to 2.30 m in height. The roof is traditionally made of fired clay corrugated tiles, placed on a mud and straw mortar layer. More recently, corrugated zinc metal sheets are used in new houses instead of corrugated clay tiles (Carazas 2001).

3. Testing facilities at PUCP

The PUCP's shaking table (Figure 7) is a 4x4 m prestressed concrete platform supported by 8 metallic vertical plates, which are pinned at both ends to allow horizontal movement. The maximum supported weight is around 150 kN. The platform is driven back and forth by a servo hydraulic actuator, which reacts against a massive concrete slab. The total displacement of the actuator is 300 mm (±150 mm).

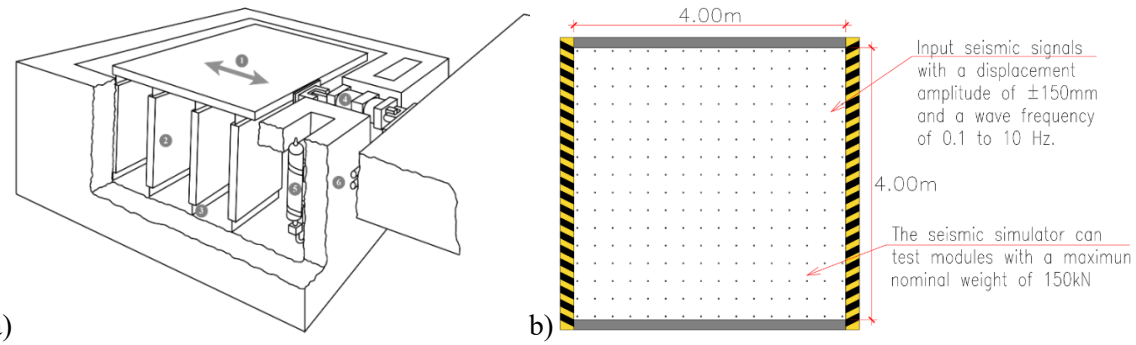

a) b)

Figure 7. Schematic view of the seismic simulator a) 3D view (modified from Esparza 1986), b) plant view

Dynamic testing of large-scale models of two-storey earthen buildings is not possible at the PUCP's shaking table, which was designed specifically to carry one-storey earthen full-scale models. Consequently, it was decided to build four half-scale two-storey models, two with mesh reinforcement and two without it.

4. Design and construction of half-scaled experimental models

4.1. Scaling process

The four identical reduced-scale adobe specimens were designed by establishing similitude ratios λ between the physical property parameters of a hypothetical full-scale *prototype* consisting of a two-storey one-room building and a half-scale *model* to be tested on the shaking table (Harris and Sabnis 1999).

The selected length scaling ratio (Prototype/Model) was λ_L= LP/LM = 2. Correspondingly, the scaling ratios for area and volume were, respectively, λ_A= 4 and λ_V= 8. Since the test models were to be made with the same soil as the real buildings, the scaling ratios used for density, modulus of elasticity and mechanical strength were set equal to 1. Therefore, the mass ratio was λ_M= λ_V= 8, and assuming that the applied stress ratio was equal to the material strength ratio (*i.e.* ignoring gravity stresses) the force ratio is equal to the area ratio (λ_F= λ_A= 4). Finally, Newton's 2nd law (F= ma) implies that an acceleration ratio λ_a= ½ and therefore, to have λ_L= 2, the time ratio must be λ_T= TP/TM= 2. Two models were unreinforced and represented typical Andean two-storey adobe houses. The other two models were reinforced with a mesh

made from nylon ropes with 1/8" nominal diameter, thus respecting the scale ratio for linear dimensions λ_L= LP/LM= 2, as a previously large-scale specimen had been reinforced with 1/4" ropes.

Therefore, the shaking table displacement command signal used was obtained by halving the amplitude of the prototype displacement command signal (LM/LP= 1/ λ_L = ½) used in previous tests, and by compressing the time scale by a factor of two (TM/TP= 1/ λ_T= ½). Figure 8 shows the final dimensions of the tested adobe models. The rope reinforcement pattern was similar to that of the one-storey models. The total weight (including the reinforced concrete foundation) for each model was around 115 kN.

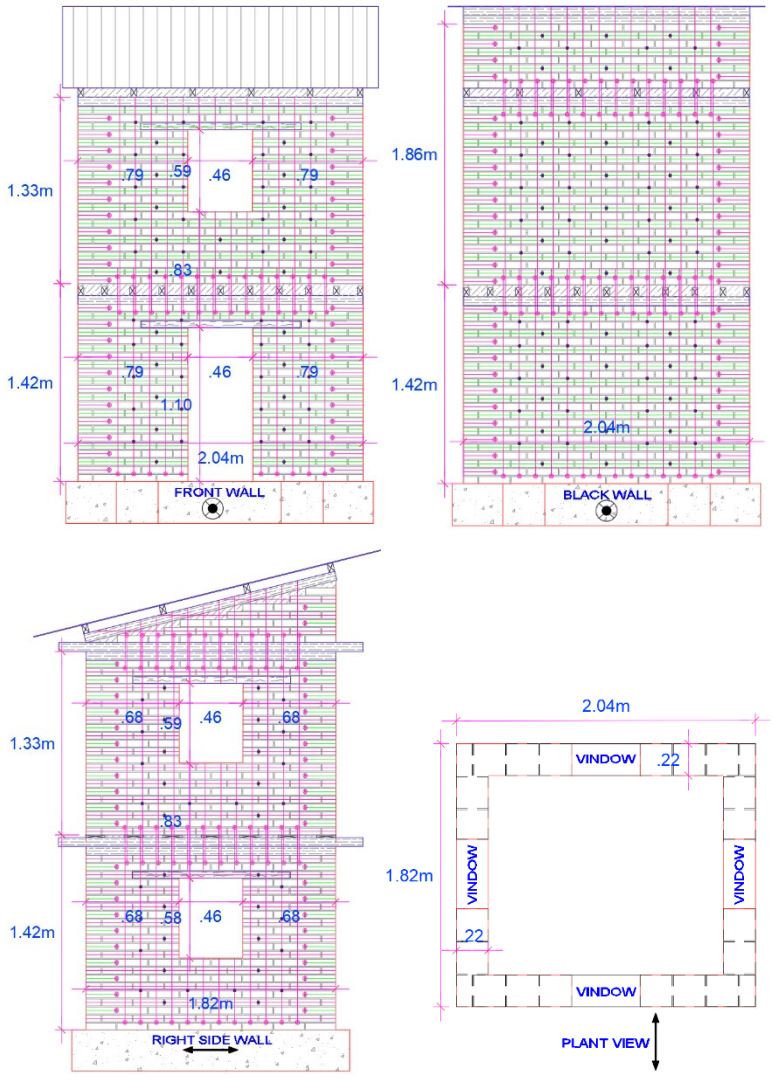

Figure 8. Mesh-reinforced reduced-scale adobe model schematics.

4.2. Construction of test specimens

The same soil was used for the fabrication of both: the adobe bricks and the mud mortar, to avoid variability in the materials. The material proportions in volume were 5:1:1 (soil:coarse sand:straw) for the adobe bricks and 1:1 (soil:coarse sand) for the mud mortar. All blocks were 221x221x50 mm and were sun-dried for at least 28 days. The four models were identical in geometry. Since the mortar thickness of actual adobe buildings range from 20 mm to 40 mm, the scaled models had 10 mm thick mortar. The lintels of doors and windows were made of cane rods tied with wire. The roofs were built using wooden boards supported on 2" x3" wooden beams. A wooden crown beam was placed at the top of each floor of all models to guarantee a boxlike behaviour. Mud stucco was applied to the exterior of the walls of the models, except for one of the reinforced models, which was left without stucco to facilitate observation of the cracks in the walls.. Each model was built on a concrete beam that was used as a foundation and as transporting base from the lab yard to the shaking table. Figure 9 shows the construction process of one unreinforced model.

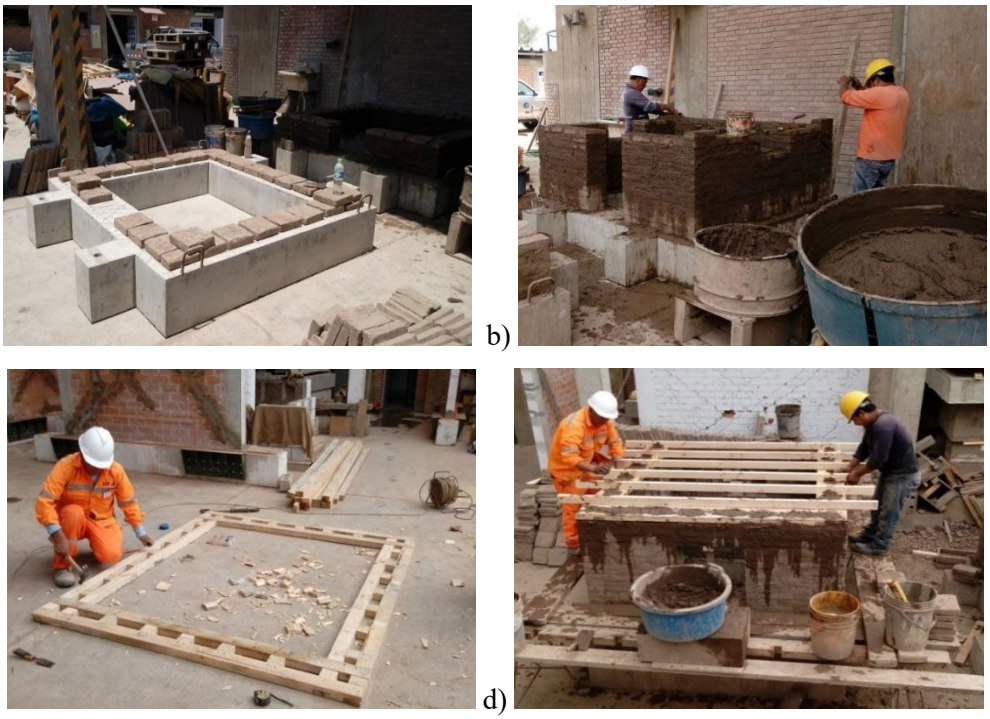

Figure 9. Construction process sequence of an unreinforced model. a) b) construction of first level walls; c) and d) installation of the wood crown beam and wood beams; e) lintels of doors and windows (made of cane rods tied with wire), f) finished model (before roof tiles placement).

Figure 9 (Continuation). Construction process sequence of an unreinforced model. a) b) construction of first level walls; c) and d) installation of the wood crown beam and wood beams; e) lintels of doors and windows (made of cane rods tied with wire), f) finished model (before roof tiles placement).

According to Blondet et al. (2016, 2019), ¼" diameter horizontal ropes are required every two adobe layers in order to reinforce one-storey adobe buildings. Then, in this work -and assuming independent failure at the first and second storey (Tomazevic 2007)- the rope reinforcement at each floor consisted of 1/8" diameter vertical and horizontal nylon ropes placed on both faces of all walls. The reinforcement spacing was consistent with the masonry layout: every two layers horizontally and every block vertically. The resulting reinforcement spacing was 0.12m horizontally and 0.11 m vertically, respectively. Holes were drilled in the mortar to allow the ropes to pass through the walls. These perforations were mainly drilled in the vertical joints close to the wall corners to place the horizontal ropes. The ropes were tied by combining an "8" knot with two simple knots, as shown in Figure 10.

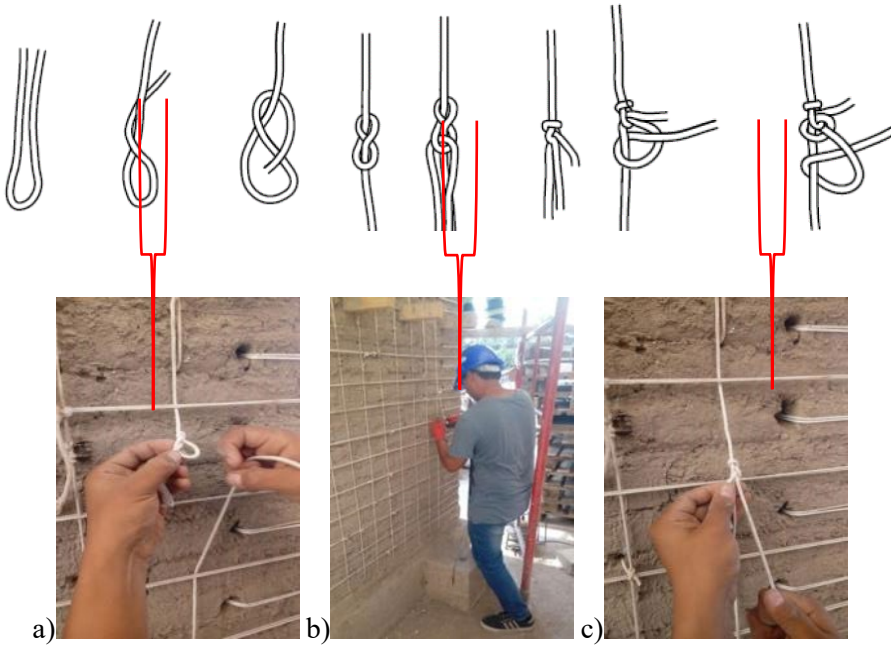

Figure 10. Joining ropes sequence: a)" 8" knot; b) rope tensioning; c) double simple knots.

The lower end of the vertical ropes was passed through holes drilled in the mortar layer between the foundation and the walls. Additional holes were drilled to connect the internal and external meshes with pass-through ropes. The first storey vertical ropes were placed first, passed over the wooden floor beams and tied to the second storey ropes. The second storey ropes passed above the wooden roof crown. Then, the horizontal ropes (which were doubled to be more conservative) were placed to form the rope mesh. The inner and outer meshes were joined with pass-through ropes. Figure 11 shows the reinforcement process of one adobe model.

Figure 11. Sequence for the reinforcement process: a) installation of vertical ropes; b) installation of horizontal ropes; c) joining of inner and outer meshes; d) reinforced adobe model.

5. Experimental program

5.1. Material properties

Preliminary control tests were performed in order to estimate the mechanical properties of the adobe masonry. These were four axial compression tests on 210 x 210 x 700 mm adobe piles and four diagonal compression tests on small square 650 x 650 x 210 mm adobe walls. The masonry samples were fabricated with 210 x 210 x 50 mm units joined with 8 to 10 mm thick mud mortar. Displacement sensors (LVDTs) were placed to measure deformations during the tests. The tests were force controlled, at 5kN/min velocity for the piles and 1 kN/min for the small walls. The mass density was 1800 kg/m3. The tests results, computed according to Norma Adobe (NTE E080 2020), are shown in Table 1.

The tensional properties of 500 mm long rope samples were measured in a universal testing machine. The tests were displacement controlled with a velocity of 10 mm/min. The maximum average tensional strength was 181.00 MPa, which corresponds to a maximum load of 1.3 kN and 0.45% elongation for each rope. The modulus of elasticity was 613 MPa with 122 MPa standard deviation.

Table 1. Elastic mechanical properties of the adobe masonry

	Mean value (MPa)	S. Deviation (MPa)
Compressive strength	1.07	0.07
Tensional strength	0.044	0.0005
Modulus of Elasticity	209.00	75.00
Shear modulus	92.00	45.00

5.2. Testing program

The seismic signal used for the dynamic tests was based on the horizontal acceleration record from the May 31st, 1970, Peruvian earthquake, component N08W recorded in Lima (seismic station of the Geophysics Peruvian Institute, IGP, Figure 12a). The corresponding acceleration spectrum is shown in Figure 12b. After digitisation, the acceleration record was windowed within the 0.10 to 10 Hz in order to stay safely below the resonant frequency of the electrohydraulic seismic simulator and to prevent amplification of low-frequency noise in the numerical double integration process. Linear baseline correction was also applied. The same unit displacement command signal was used for all tests, multiplying its amplitude by the desired peak table displacement, according to Table 1.

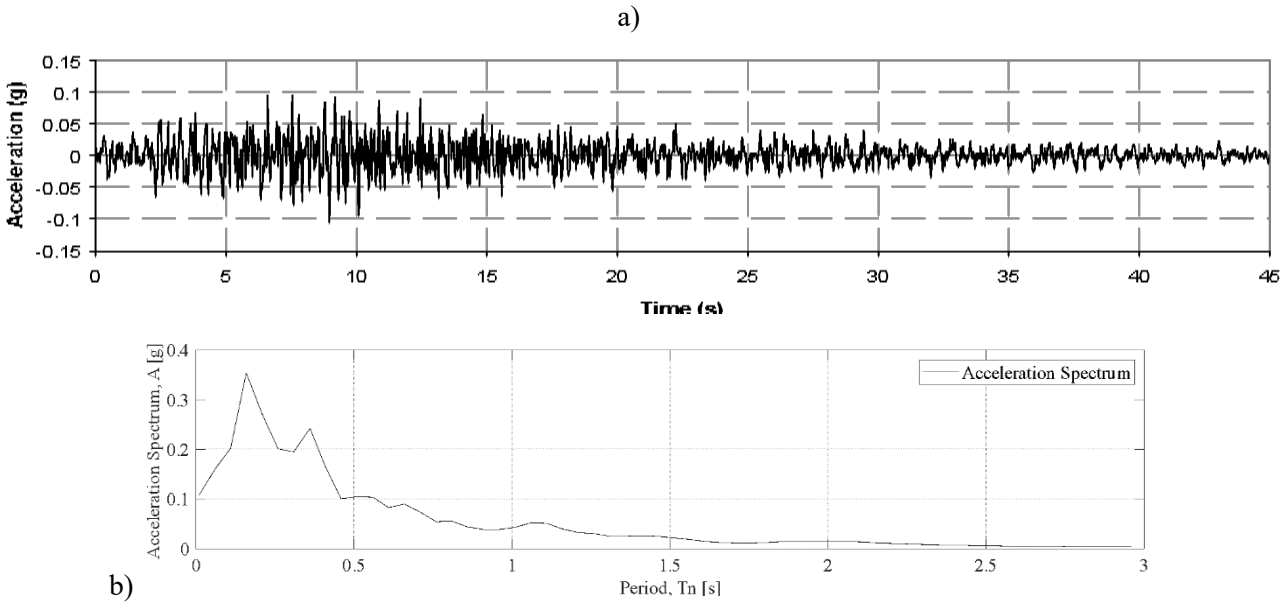

Figure 12. a) Horizontal acceleration record from May 1970 Peruvian earthquake, component N08W, registered in Lima. b) Acceleration response spectrum.

The following nomenclature was used to identify the test specimens: URM-N for Unreinforced Model N and SRM-N for String Reinforced Model N. Table 2 summarizes the command peak displacement $D0_{max}$ and the expected peak table acceleration $A0_{max}$ for this testing campaign. It was considered that a peak table displacement smaller than 15 mm would represent a light earthquake; that between 30 and 45 mm, a moderate earthquake; and that greater than 60 mm, a strong earthquake. Although the platform movements are unidirectional, the damage inflicted on all adobe models tested previously was consistent with that observed in the field during real earthquakes, and thus it is considered that these tests provide realistic simulation of seismic action.

Table 2. Summary of tests performed and peak motion values expected.

Table motion intensity	**$D0_{max}$**	**$A0_{max}$**	**URM-1**	**URM-2**	**SRM-1**	**SRM-2**
Light	15.0 mm	0.50 g	✓		✓	
Moderate	30.0 mm	1.00 g	✓		✓	
	37.5 mm	1.12 g	✓			
	45.0 mm	1.27 g		✓		
Strong	60.0 mm	1.68 - 1.75 g		✓	✓✓	✓✓
	90.0 mm	2.20 g		✓		

Each model was placed on the shaking table with the window walls parallel to the platform movement (Figure 13). Figure 14 summarizes the instrumentation used to record the model response. It consisted of 11 LVDT displacement sensors (D1 to D11), 10 accelerometers (A1 to A10) and 2 load cells (L1 and L2) placed within selected horizontal ropes. Additionally, the force applied by the actuator (F0) and the table displacement and acceleration (D0, A0, respectively) were recorded.

Figure 13. Panoramic view of two adobe models on the shaking table.

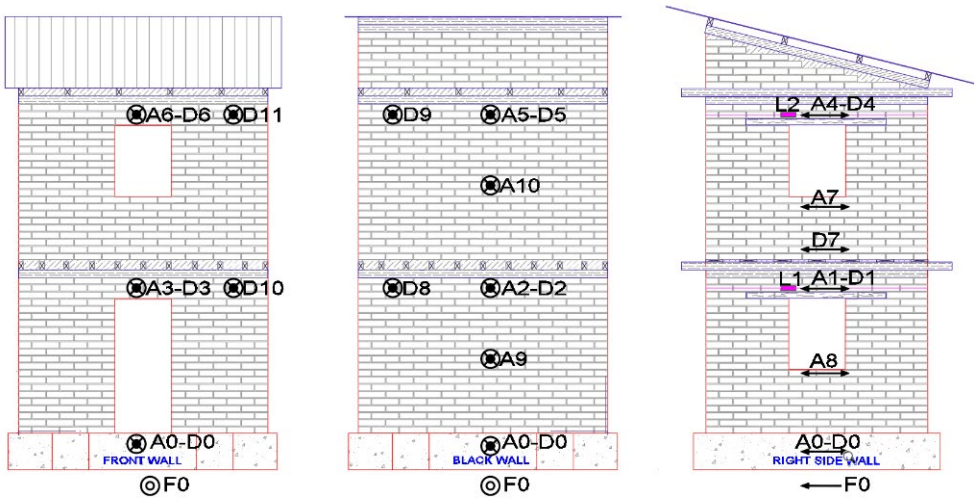

Figure 14. Distribution of LVDTs (D), accelerometers (A) and load cells (L).

5.3. Experimental tests

The seismic signal was perpendicular to the front (with door) and back (without openings) walls, and parallel to the lateral walls (with windows). During the light simulated seismic movement ($D0_{max}$= 15 mm and $A0_{max}$= 0.5g), the model without reinforcement URM-1 showed some slight cracks in the stucco on the first floor (Figure 15a,b,c) and almost no visible damage on the second floor. Also, some horizontal fissures at the slab levels and at the first floor front wall were observed (Figure 13a,b), indicating out-of-plane actions. The reinforced model SRM-1 showed superficial cracks just in the stucco (Figure 13d,e). Intentionally, some parts of the adobe walls were left without stucco in the SRM-1 to visualize the damage on walls and nylon ropes after each shake.

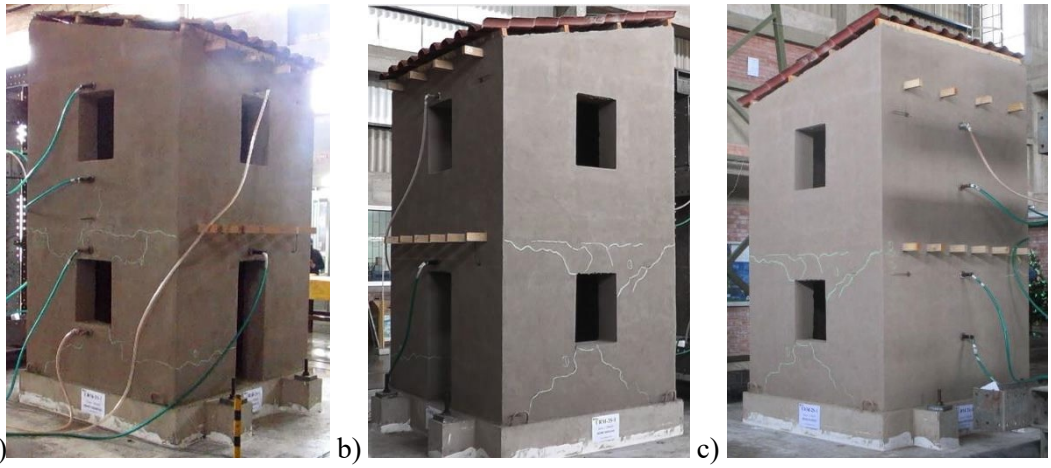

Figure 15. Adobe models after light shake: a), b), c) Unreinforced model; d), e) Reinforced model.

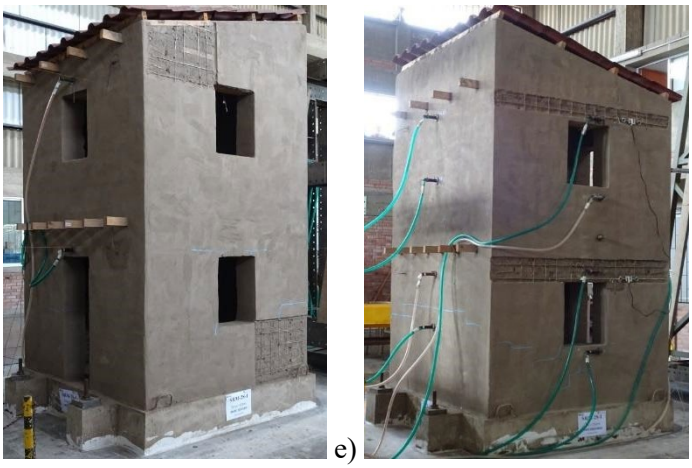

d) e)

Figure 15. (Continuation) Adobe models after light shake: a), b), c) Unreinforced model; d), e) Reinforced model.

During the moderate seismic motion ($D0_{max}$= 30 mm and $A0_{max}$= 1.0g), the unreinforced model URM-1 suffered visible diagonal cracking on the lateral walls at both levels (Figure 16a,b). Also, horizontal cracks could be observed at the mid-height of the second storey (especially at the front wall) and the base of the sloped roof. At the end of the movement, the first floor back wall suffered a slight rotation due to the out-of-plane actions (Figure 16b,c). At this stage, the building almost lost its structural stability. In the reinforced model SRM-1, some small horizontal cracks appeared at the mid-height of the first floor at the front and back walls, and slightly diagonal cracks at the first-storey walls parallel to the movement (Figure 16d,e).

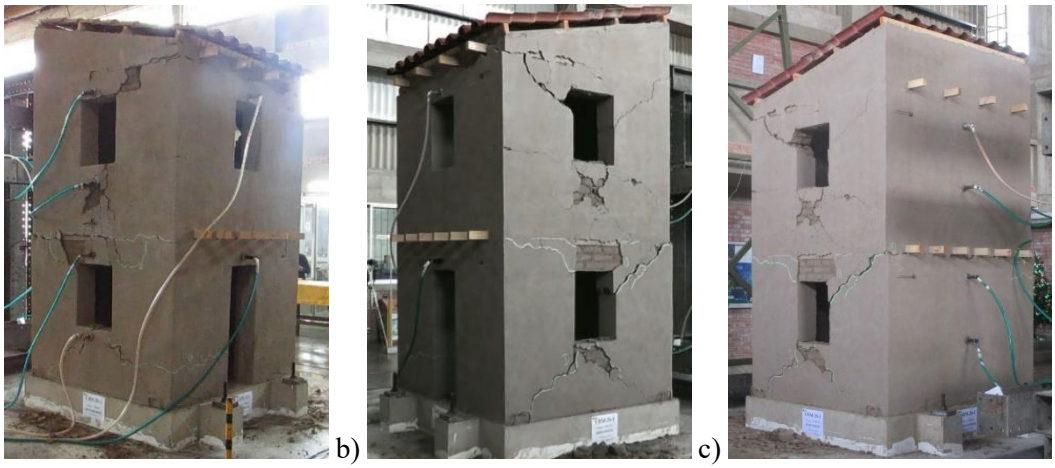

a) b) c)

Figure 16. Adobe models after moderate shake: a), b), c) Unreinforced model; d), e) Reinforced model.

d)  e) 

Figure 16. (Continuation) Adobe models after moderate shake: a), b), c) Unreinforced model; d), e) Reinforced model.

During the strong seismic motion ($D0_{max}$= 60 mm and $A0_{max}$= 1.68 g), the unreinforced model URM-2 model was close to collapse. The front first and second storey walls were separated from the floor beams due to the out-of-plane actions (Figure 17a,b), and each of them seemed to behave independently of each other. Thick diagonal cracks were formed on the second storey back wall, across the full wall thickness (Figure 17c). Diagonal cracks in the lateral walls increased and there was a clear separation between the walls and the sloped roof. If there were no wooden collar beams on each floor, then the first and second storey walls could have behaved as a single wall, and the overturning could have occured with the axis of rotation placed at the bottom of the first storey wall, as has been reported in some damage studies of other URM structures (Adhikari and D'Ayala 2020, Varum et al. 2018).

In the reinforced model SRM-2 (which had no stucco), horizontal cracks formed near the base of the first-storey front and back walls, and at the mid-height and top part of the second storey front wall. Also, the thickness of the diagonal cracks at the first-storey walls (parallel to the movement) increased. With this, some wall portions were formed; however, the rope mesh reinforcement was able to hold all these wall parts together. During the second strong shaking, a rocking motion of the wall pieces was observed, but again the rope mesh avoided the collapse of the structure. The cracks formed in the preliminary motion opened more, allowing more energy dissipation. Some adobe crushing was also observed below the windows of the second level (Figure 17d,e).

Figure 17. Two-storey models after a strong motion: a), b), c) Unreinforced model; d), e) Reinforced model.

In all the models (URM and SRM), wooden collar beams were placed above each floor. Unlike URM structures with no collar beams, here the overturning of the first and second-storey floor of the URM front and back walls behave independently of each other. This means that the rocking mechanism of the second floor walls does not depend on the movement of the first floor wall. According to Adhikari and D'Ayala (2020) and Varum et al. (2018), when there are no collar beams, then the first and second floor walls overturn as they were one tall wall.

5.4. Dynamic properties

All the test specimens were subjected to base displacement pulses to induce free vibration motions before and after each seismic movement (Figure 18). The natural period of each model was computed by analyzing the acceleration records of each wall and the damping ratio by using logarithmic decrement method (Chopra 2017). Figure 19 shows an example of the free vibration acceleration response of one unreinforced wall.

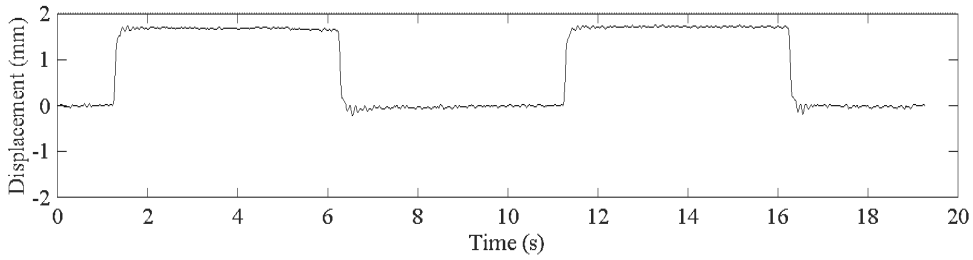

Figure 18. Rectangular pulse for free vibration movement.

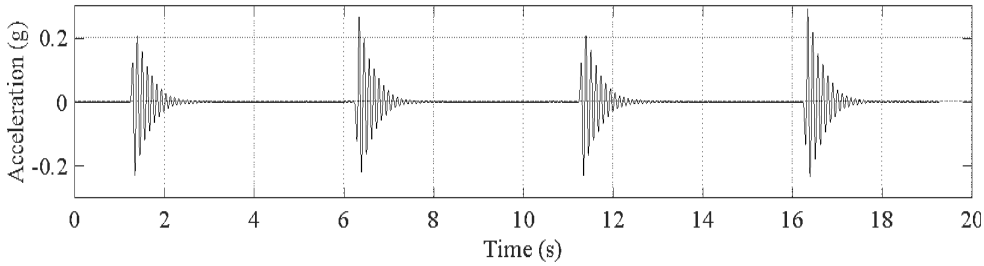

Figure 19. Acceleration record of one unreinforced lateral wall obtained during free vibration tests.

Table 3 summarizes the computed dynamic properties of the unreinforced and reinforced models. The initial natural period of the first unreinforced model was around 0.13 s. After the light seismic motion, the model experienced minor damage, and did not change its natural vibration period. The first model, reinforced with rope mesh initially was slightly stiffer, with a natural vibration period of 0.11 s, but after the light seismic motion, its period increased to 0.14 s due to slight cracking of the adobe masonry. Predictably, the natural period of both models increased after each test due to the stiffness degradation caused by seismic cracking on the adobe walls. Whereas the period of the unreinforced model increased by more than 300% (from 0.13 s to 0.53 s) the corresponding natural period increase for the reinforced model was about 170%, which is consistent with the significantly larger extent of damage suffered by the unreinforced model. The evolution of equivalent viscous damping ratio as measured on the first floor is more difficult to interpret. The general trend indicates that the URM walls presented more energy dissipation than the SRM walls, except during the moderate shake.

Table 3. Dynamic properties of the URM and SRM models.

a) Period of vibration

	Tn (s)			
	Initial	**Light shake**	**Moderate shake**	**Strong shake**
URM	0.13	0.13	0.35	0.53
SRM	0.11	0.14	0.25	0.30

b) Equivalent viscous damping

	ξ (%)							
	Initial		Light shake		Moderate shake		Strong shake	
	1st level	2nd level	1st level	2nd level	1st level	2nd level	1st level	2nd level
URM	9.70	7.45	9.90	7.10	16.35	13.30	16.80	14.60
SRM	5.50	5.55	9.30	6.90	20.50	12.45	13.50	11.10

6. Test results

Measured peak values of some response parameters for all the models for light, moderate and strong shaking are summarized in Table 4. Inter-storey drift ratios (IDRs) are shown because they are related to damage and do not depend on scale.

Table 4. Summary of measured peak values.

Model ID	Shaking intensity	Table		Base shear V (kN)	Rope force F (kN)
		displacement D0 (mm)	acceleration A0 (g)		
URM-1	Light	15 mm	0.5 g	44.5	-
SRM-1				44.0	0.13
URM-1	Moderate	30 mm	1.0 g	66.7	-
SRM-1				58.9	0.30
URM-2	Strong	60 mm	1.68 g	68.9	-
SRM-1				83.6	0.57
SRM-2			1.75 g	90.0	0.19

Table 4. (Continuation) Summary of measured peak values.

Model ID	Shaking intensity	Lateral wall (D1, D4)				Back wall (D2, D5)				Front wall (D3, D6)			
		Relative displacement (mm)		Inter-storey drift ratios (‰)		Relative displacement (mm)		Inter-storey drift ratios (‰)		Relative displacement (mm)		Inter-storey drift ratios (‰)	
		1st level	2nd level	1st level	2nd level	1st level	2nd level	1st level	2nd level	1st level	2nd level	1st level	2nd level
URM-1	Light	4.5	8.7	3.6	6.3	6.3	4.3	5.3	2.8	5.0	4.3	4.2	2.8
SRM-1		4.1	5.7	3.3	4.1	5.3	4.7	4.5	3.1	4.7	4.7	4.0	3.1
URM-1	Moderate	64.8	64.7	52.3	46.5	38.1	37.9	32.2	24.9	30.8	30.8	26.0	20.3
SRM-1		13.9	21.5	11.2	15.5	14.0	21.5	11.8	14.1	13.8	20.4	11.6	13.4
URM-2	Strong	41.7	-	33.6	-	58.8	56.7	49.6	37.3	33.2	-	28.0	-
SRM-1		32.8	48.4	26.5	34.8	42.2	38.9	35.6	25.6	29.1	40.1	24.6	26.4
SRM-2		33.7	47.0	27.2	33.8	58.5	52.2	49.4	34.3	46.3	33.3	39.1	21.9

From the measurements presented in Table 4, it can be inferred that unreinforced models suffered considerably more damage than the string-reinforced models, thus validating the efficacy of the reinforcement provided. For example, the IDR in the lateral walls of the unreinforced model URM-1 increased 15 times from light to moderate shake on the first level and almost 7.5 times on the second level.

For the front and back walls of the URM-1, the IDR increased 6.5 and 8 times for the first and second levels, respectively. The reinforced models showed significant lower IDRs. For example, for the first reinforced model, the IDR increased 3 times on the first level and 4.2 times on the second one. Also, all the IDRs for walls on the same level in the SRM-1 were similar, indicating that the string reinforcement also helped to have a box behaviour for the complete structure.

The effectiveness of the rope reinforcement in reducing seismic damage can be furthermore assessed by comparing the peak lateral displacement of the unreinforced model walls with those of the reinforced models. For instance, rope reinforcement was able to reduce the maximum lateral displacement at the moderate shaking in the SRM-1 by 4.6 times for the first level and 3 times for the second level, in comparison with the URM-1. For the front and back walls, subjected to out-of-plane actions, the peak displacements were reduced by 2.5 and 1.6 times for the first and second levels, respectively.

Some LVDTs placed on the second floor of the URM-2 model were removed before the strong shaking test in order to prevent their damage. For the strong shaking and for the SRM-2 first level lateral walls, it is seen that the strings reduced in 25% the maximum lateral displacements compared with those of the URM-2. However, for the back walls, almost the same maximum relative displacements were reached at the URM-2 and SRM-2, first and second level.

The computed values of peak base shear during the strong movement reveal that the rope reinforcement contributed to increase the lateral strength of the models by about 17%, without losing stability. At this point, the maximum registered force at the rope was 0.57 kN at the first level. Since the ultimate strength of the ropes was 1.4 kN, they did not reach their maximum capacity.

Figures 20 and 21 show the time history records of relative displacements of the back wall of all models, together with the base acceleration for moderate and strong shaking ($D0_{max}$= 30 mm and $D0_{max}$= 60 mm, respectively). Damage to the unreinforced adobe models is evidenced by the permanent residual deformations, while the string-reinforced adobe models return almost to their original positions.

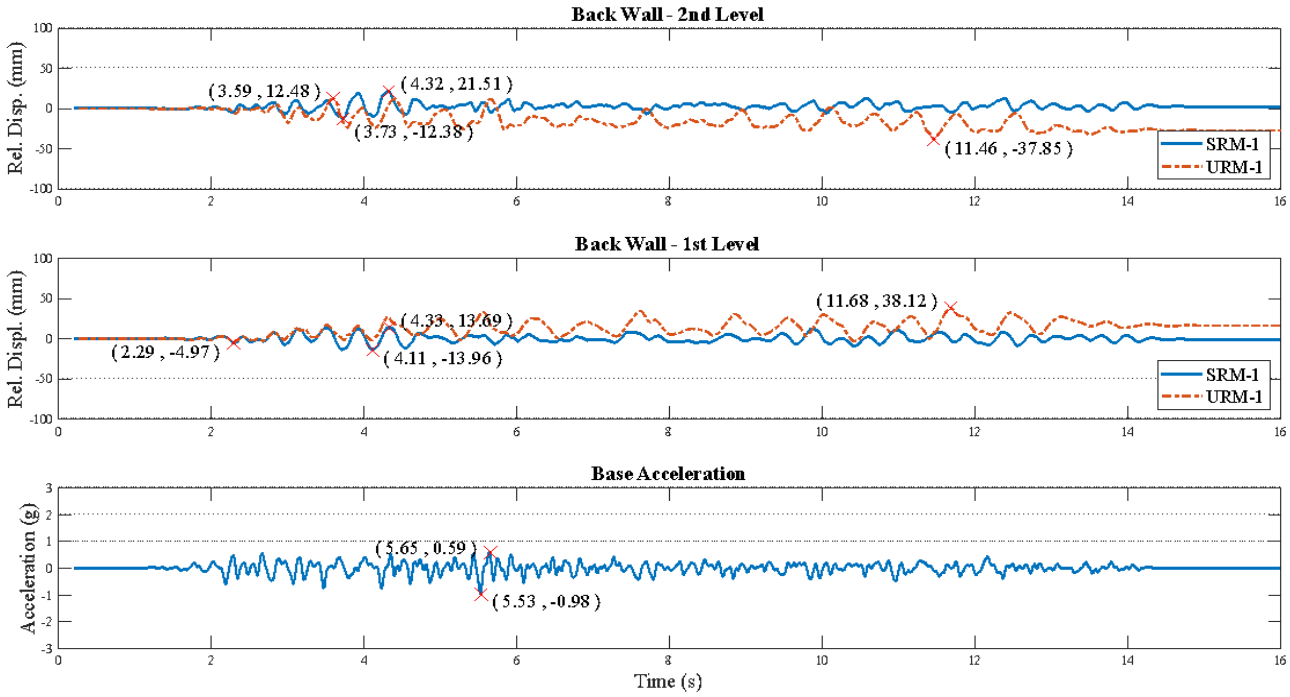

Figure 20. Back wall inter-storey displacements of URM-1 and SRM-1 for moderate shaking ($D0_{max}$= 30 mm, $A0_{max}$= 1.00g).

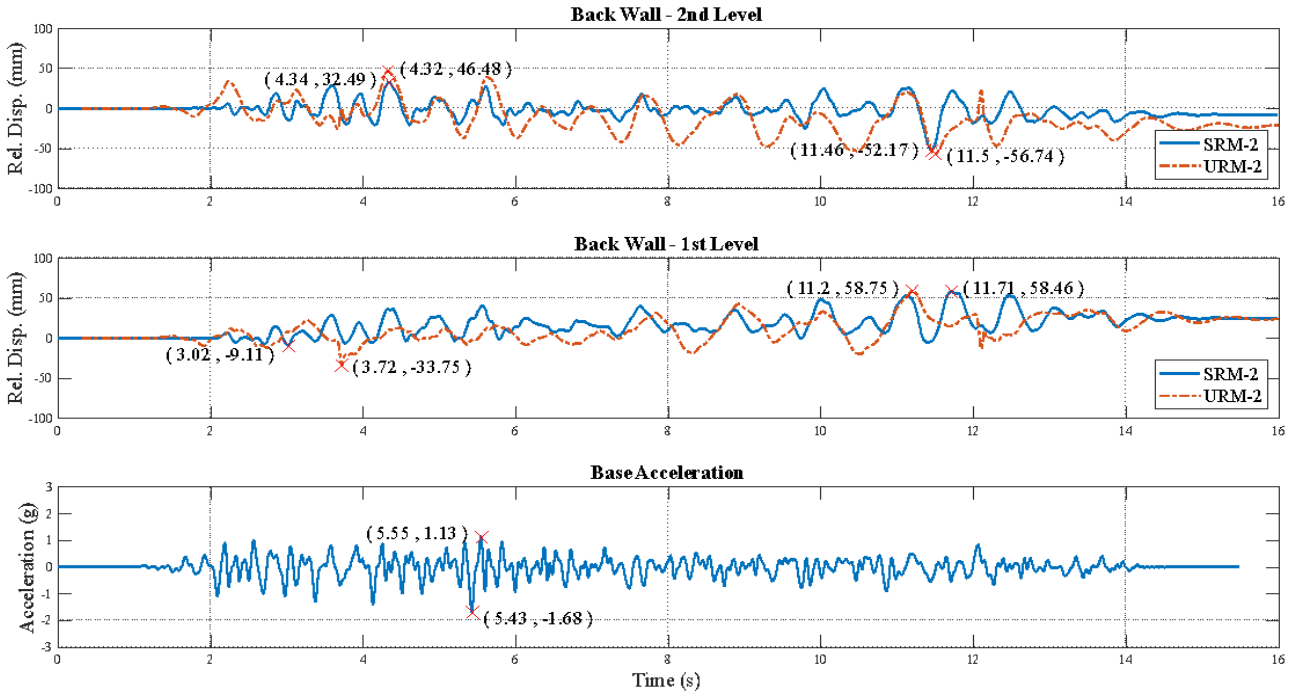

Figure 21. Back wall inter-storey displacements of URM-2 and SRM-2 for strong shaking ($D0_{max}$= 60mm, $A0_{max}$= 1.68g).

Figure 22 shows back wall displacement profiles of unreinforced model URM-2 and string-reinforced model SRM-2 for a strong shake at specific times. The blue dashed line shows the displacement profile at 6 s, which is the time when the maximum acceleration amplitude (PGA) was registered. The orange dashed line shows the residual displacement profiles at the end of the test. It is observed that the second storey relative displacements of the unreinforced model (Figure 22a) are greater than the relative displacements at the reinforced model. For example, the relative displacement at 15 s for the URM-2 second level was almost 25 mm, while for the SRM-2 was less than 5 mm (Figure 22b). Although the relative displacements for the unreinforced and reinforced models on the first storey were almost the same, the string reinforcement controlled the structural stability of the SRM-2.

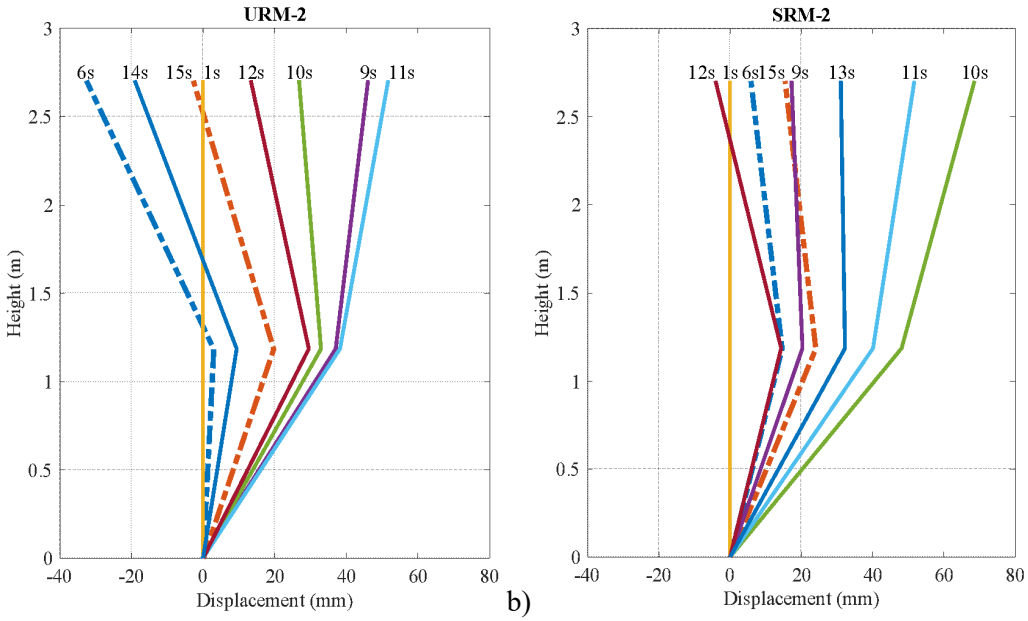

a) b)

Figure 22. Profiles of back wall displacement at selected instants of a strong shake (D0max=60 mm and A0max= 1.68g): a) unreinforced model, b) reinforced model.

Figures 23, 24 and 25 present the shear vs first-floor displacement curves (back walls) for unreinforced model and reinforced model during light, moderate and strong ground motions, respectively. During light shaking (Figure 23), the hysteretic curve of the URM does not show a linear trend, thus indicating significant structural damage and incursion in the inelastic range. The SRM, however, shows a narrower hysteretic curve from which an average lateral stiffness of 1 840 kN/mm was estimated.

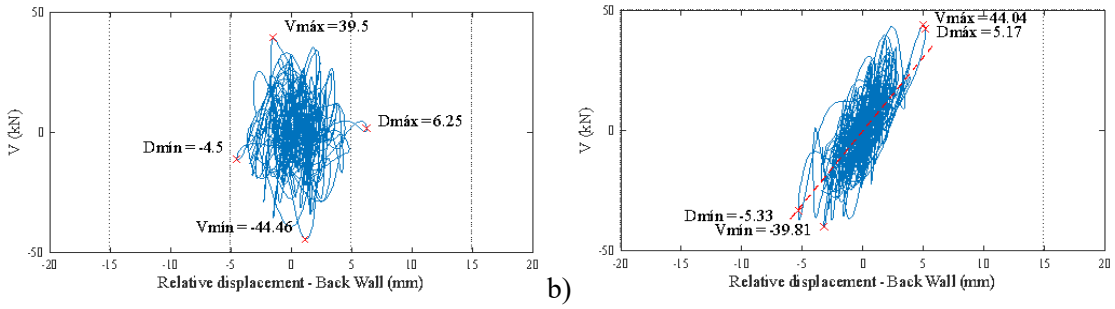

a) b)

Figure 23. First storey Base shear vs displacement curves measured: a) URM-1 and b) SRM-1 for ($D0_{max}$= 15mm).

During moderate ground motions (Figure 24), the hysteretic curves of the reinforced model still show a linear trend, indicating an elastic response component due to the action of the rope mesh. This occurred because the elastic ropes prevented relative displacements between the different wall portions, thus preserving structural integrity. As expected, the URM force-displacement response was irregular, which indicates significant structural damage.

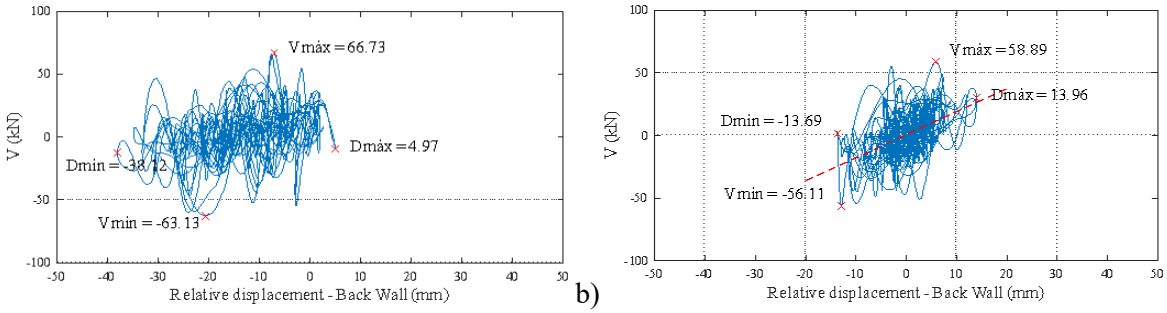

a) b)

Figure 24. Base force vs top displacement curves measured at back walls (1st level) of a) URM-1 and b) SRM-1 for a moderate motion ($D0_{max}$= 30mm).

Finally, a comparison of the lateral force-displacement response shown by models URM-2 and SMR-1 during strong shaking (Figure 25) reveals that the rope meshes reduced displacement on the first storey level. The reinforced model resisted about 25% more peak lateral force with less than 30% peak lateral displacement than the unreinforced one (see Table 4). The linear trend shown by the hysteretic curves of the reinforced model indicates that the model is still stable. The irregular shape of the hysteretic curve of the URM-2 indicates that this model lost its structural stability, showing large displacements at much lower loads compared to those recorded in the reinforced models.

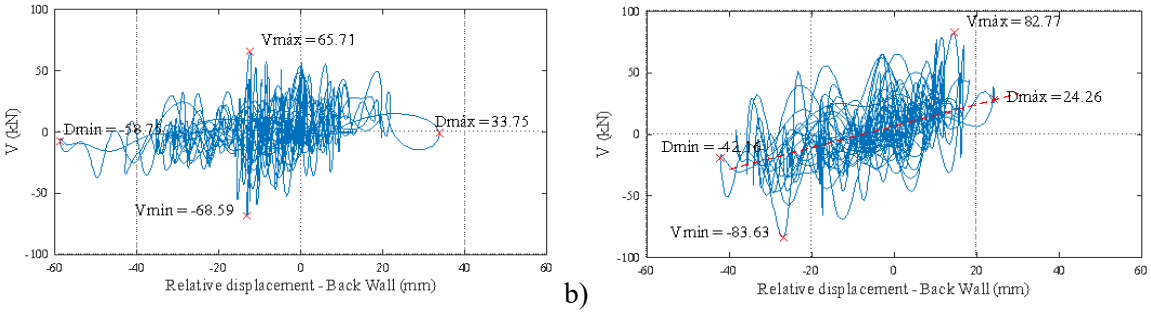

a) b)

Figure 25. Base force vs top displacement curves measured at back walls (first storey) of a) URM-2; b) SRM-1for a strong motion ($D0_{max}$= 60mm).

Finally, Figure 26 shows the first storey lateral force-displacement envelopes for all models (Blondet et al. 2013). For each structure, the base shear was divided by the mass of the whole structure to compute the pseudo-acceleration Sa. Three points (A, B and C) were then identified in the relative displacement versus pseudo acceleration graph. Point A corresponds to the displacement at which the elastic behaviour is lost, point B indicates the beginning of significant nonlinear response and point C indicates the stage of strength deterioration.

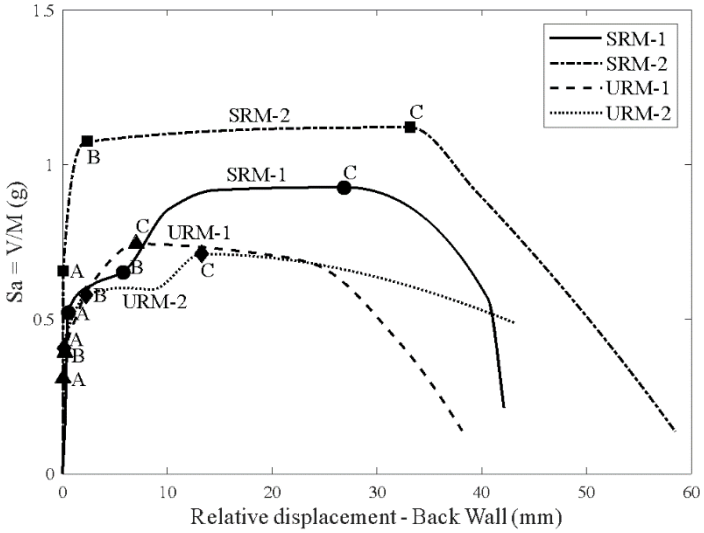

Figure 26. Lateral force vs relative displacement envelope – first storey back walls.

The curves in Figure 26 show that the nylon mesh increased the maximum lateral capacity of the SRM-1 and SRM-2 by 50% and 80%, respectively, compared to the unreinforced models. Since the first reinforced model was subjected to the light, moderate and strong shake, its lateral capacity is less than the second reinforced model, which was just subjected to a strong shaking. The curve of the SRM-2 in Figure 26 was computed considering only the first strong shake. The difference in lateral capacity in the reinforced models

shows the importance of considering also cumulative damage in the adobe buildings when analyzing their seismic performance. Small tremors may also decrease the lateral strength of the adobe constructions. Displacements at the maximum lateral force (point C) were greater for the reinforced models. This is an indication of the increment in the displacement ductility of the reinforced models, having more floor relative displacements with less damage. At the end of the tests, both reinforced models were structurally stable, while the unreinforced models collapsed.

7. Conclusions

The main conclusions that can be drawn from this experimental project are as follows:

- The two reduced-scale unreinforced two-storey adobe models tested on the PUCP's shaking table showed a seismic response consistent with that observed in the field: they suffered significant structural damage and became unstable during moderate ground shaking and collapsed catastrophically during strong ground motions.
- The research project was successful because it demonstrated that the proposed nylon mesh reinforcement provided seismic safety to two-storey adobe models, as was demonstrated previously for one-story adobe models. The nylon mesh was capable of holding together the wall portions broken by the seismic action, thereby maintaining the structural integrity of the buildings.
- The reduced-scale reinforced adobe models showed consistently better seismic response than their unreinforced counterparts. The rope reinforcement provided additional energy dissipation capacity, and higher lateral stiffness and strength to the adobe walls. Most importantly the reinforcement preserved the structural integrity and avoided the collapse of the building models.
- The nylon ropes used to reinforce the adobe models are widely available in the Andean regions at an affordable cost to the local dwellers. It seems feasible, therefore, that this system could be used to provide seismic safety to many living in seismic regions.

The extensive research effort developed over the years at the PUCP and other institutions has demonstrated that the construction of earthquake-resistant earthen buildings is feasible. However, it is necessary to develop engineering design methods to optimise the amount and configuration of the reinforcement required.

The technical solution described here, unfortunately, is not sufficient to solve the real problem of the unacceptable seismic risk for the millions of inhabitants of earthen houses. Mitigation of seismic risk will be possible only with the support of the governmental and non-governmental institutions, combined with

extensive programs of technology transfer and construction training to the users themselves, until they adopt improved earthen construction systems as part of their own culture.

8. Acknowledgements

The authors would like to thank SENCICO, a Peruvian government institute devoted to construction code development and training, for the funding provided along with the experimental tests. Also, the support of the Structures Laboratory technical staff is gratefully acknowledged. Finally, our thanks to all the students and colleagues who participated in this research.

9. Declarations

Not applicable.

10. References

Adhikari R, D'Ayala D (2020) 2015 Nepal Earthquake: Seismic Performance and post-earthquake reconstruction of stone in mud mortar masonry buildings. Bulletin of Earthquake Engineering 18:3863-3896.

Avrami E, Guillaud H, Hardy M (eds) (2008) Terra literature review: An overview of research in earthen architecture conservation. The Getty Conservation Institute, California, USA.

Berge B. The ecology of building materials (2nd ed) (2009). Architectural Press, Elsevier Science.

Blondet M, Torrealva D, Villa-García G, Ginocchio F and Madueño I (2005) Using Industrial Materials for the Construction of Safe Adobe Houses in Seismic Areas. Proceedings of SismoAdobe 2005. Pontifical Catholic University of Peru, Lima, Peru.

Blondet M, Vargas J, Tarque N, Iwaki C (2011) Construcción Sismorresistente en tierra: la gran experiencia contemporánea de la Pontificia Universidad Católica del Perú (in Spanish). Journal of Informes de la Construcción, Vol. 63, 523, pp 41-50.

Blondet M, Vargas J, Sosa C A, Soto E J (2013) Seismic simulation tests to validate a dual technique for repairing adobe historical buildings damaged by earthquakes. KERPIC2013: New Generation Earthen Architecture: Learning from Heritage, 11-14 September 2013. Istanbul Aydin University. Istanbul, Turkey.

Blondet M, Vargas J, Tarque N, Soto J, Sosa C, Sarmiento J (2016) Seismic protection of earthen vernacular and historical constructions. Proceedings of the 10th International Conference on Structural Analysis of Historical Constructions, SAHC2016, (pp. 3-14) CRC Press, ISBN 9781138029514, Lovaina, Belgium.

Blondet M, Tarque N, Vargas J, Vargas H (2019) Evaluation of a rope mesh reinforcement system for adobe dwellings in seismic areas. Proceedings of the 11th International Conference on Structural Analysis of Historical Constructions. September 10-13, Cusco, Peru.

Bossio S, Blondet M, Rihal S (2013) Seismic behavior and shaking direction influence on adobe wall structures reinforced with geogrid. Earthq. Spectra 2013;29(1):59–84.

Brando G, Cocco G, Mazzanti C, Peruch M, Spacone E, Alfaro C, Sovero K, Tarque N (2019) Structural survey and empirical seismic vulnerability assessment of dwellings in the historical center of Cusco, Peru. International Journal of Architectural Heritage. Article in Press.

Carazas W (2001) Vivienda Urbana Popular de adobe en el Cusco, in Spanish, UNESCO, Grenoble, France.

Chopra A. Dynamics of Structures (5th edition) (2017). Pearson.

Correia M (2016) Conservation in Earthen Heritage — Assessment and Significance of Failure, Criteria, Conservation Theory, and Strategies. Cambridge Scholars Publishing, UK.

Costa A, Miranda J, Varum H (2014) Structural Rehabilitation of Old Buildings, Ch: Structural Behaviour and Retrofitting of Adobe Masonry Buildings. Springer, 1st edition.

Dowling D (2004) Adobe housing in El Salvador: Earthquake performance and seismic improvement. In: Rose, I., Bommer, J.J., López, D.L., Carr, M.J., Major, J.J. (eds.) Natual hazards in El Salvador. Geological Society of America Special Papers, pp. 281–300.

Easton D (2007) The Rammed Earth House. J. Barstow (ed), Chelsea Publishing Company, Vertmon, USA, p. 266.

Esparza C (1986). Efectos de Interacción Estructura -Mesa vibradora- durante Ensayos de Simulación Sísmica. Master Thesis. Pontificia Universidad Católica del Perú. Lima, Peru.

Figueiredo A, Varum H, Costa A, Oliveira C (2013) Seismic retrofitting solution of an adobe masonry wall. Mater. Struct. 2013;46(1–2):203–219.

Harris H, Sabnis G. Structural modeling and experimental techniques (1st edition) (1999). CRC Press.

Houben H, Guillaud H (1994) Earth Construction: A comprehensive Guide. Intermediate Technology Publication, London, UK.

Illampas R, Silva RA, Charmpis DC, Lourenço PB, Ioannou I (2017) Validation of the repair effectiveness of clay-based grout injections by lateral load testing of an adobe model building. Constr. Build. Mater. 2017:153:174–184.

Ismail N, Khattak N (2016) Building typologies prevalent in Northern Pakistan and their performance during the 2015 Hindu Kush earthquake. Earthq. Spectra 2016;32(4):2473–2493.

Khan F, Ahmad M, Ahmad N (2021) Shake table testing of confined adobe masonry structures. Earthquakes and Structures 2021; 20(2):149-160.

Lacouture LE, Phillips Bernal C, Ortiz R, Carlos J, Ruiz Valencia D. Estudios de vulnerabilidad sísmica, rehabilitación y refuerzo de casas en adobe y tapia pisada. Apuntes 2007;20(2):286–303.

Müller U, Miccoli L, Fontana F (2016) Development of a lime based grout for cracks repair in earthen constructions. Constr. Build. Mater. 2016;110(1):323–332.

NTE E080 (2020) Norma Técnica de Edificación, Adobe Peruvian Code, Ministerio de Vivienda, Construcción y Saneamiento. Resolución Ministerial N121-2017 Vivienda.

Parisi F, Iovinella I, Balsamo A, Augenti N, Prota A (2013) In-plane behaviour of tuff masonry strengthened with inorganic matrix-grid composites. Composites Part B: Eng. 2013;45(1):1657–1666.

Parisi F, Asprone D, Fenu L, Prota A (2015) Experimental characterization of Italian composite adobe bricks reinforced with straw fibers. Composite Struct. 2015;122:300–307.

Parisi F., Blondet M., Charleson A., Varum H (2021) Seismic Strengthening Techniques for Adobe Construction. In: Varum H., Parisi F., Tarque N., Silveira D. (eds) Structural Characterization and

Seismic Retrofitting of Adobe Constructions. Building Pathology and Rehabilitation, vol 20. Springer, Cham. https://doi.org/10.1007/978-3-030-74737-4_8.

Reyes C, Smith-Pardo J, Yamin L, Galvis F, Angel C, Sandoval J, Gonzalez C (2019) Seismic experimental assessment of steel and synthetic meshes for retrofitting heritage earthen structures. Eng Struct 198: https://doi.org/10.1016/j.engstruct.2019.109477.

San Bartolomé Á, Delgado E, Quiun, D (2009) Seismic Behaviour of Two Story Model of Confined Adobe Masonry. Proceedings of the Eleventh Canadian Masonry Conference.Toronto, Canada.

Silva RA, Schueremans L, Oliveira DV (2009) Grouting as a repair/strengthening solution for earth constructions. In: Proceedings of 1st WTA international PhD symposium, WTA publications, Leuven, Belgium, pp 517–535.

Silva RA, Schueremans L, Oliveira DV, Dekoning K, Gyssels T (2012) On the development of unmodified mud grouts for repairing earth constructions: rheology, strength and adhesion. Mater Struct 45:1497–1512.

Sumerente G, Lovon H, Tarque N, Chácara C (2020) Assessment of combined in-plane and out-of-plane fragility functions for adobe masonry buildings in the Peruvian Andes. Frontiers in Built Environment, 2020, 6, 52.

Tarque N, Crowley H, Varum H, Pinho R (2012) Displacement-Based Fragility Curves for Seismic Assessment of Adobe Buildings in Cusco, Peru. Earthquake Spectra Journal, Volume 28, No. 2, pages 759–794.

Tarque N, Camata G, Spacone E, Varum H, Blondet M (2014a) Numerical simulation of an adobe wall under in-plane loading. Earthquakes and Structures, Volume 6, Issue 6, pages 627-646.

Tarque N, Camata G, Spacone E, Varum H and Blondet M (2014b) Non-linear dynamic analysis of a full-scale unreinforced adobe model. Earthquake Spectra Journal. Volume 30, No. 4, pages 759–794.

Tarque N, Sayın E, Rafi M, Tolles E (2021) Behaviour of Adobe Construction in Recent Earthquakes. In: Varum H., Parisi F., Tarque N., Silveira D. (eds) Structural Characterization and Seismic Retrofitting of Adobe Constructions. Building Pathology and Rehabilitation, vol 20. Springer, Cham. https://doi.org/10.1007/978-3-030-74737-4_2.

Tomazevic, M (2007) Damage as a measure for earthquake-resistant design of masonry structure: Slovenian experience. Can. J. Civ. Eng. 34:1403-1412.

Torrealva D, Vargas J, Blondet M (2006) Earthquake Resistant Design Criteria and Testing of Adobe Buildings at Pontificia Universidad Católica del Perú. Proceedings of GSAP Colloquium. GGI-Getty. California, USA.

Vargas J, Blondet M, Ginocchio F, Morales K, Iwaki C (2008) Uso de grouts de barro líquido para reparar fisuras estructurales en muros históricos de adobe. In: Proceedings of V Congresso de Tierra en Cuenca de Campos, Valladolid, Spain.

Varum H, Dumaru R, Furtado A, Barbosa A, Gautam D, Rodrigues H (2018) Seismic Performance of Buildings in Nepal After the Gorkha Earthquake. Impacts and Insights of Gorkha Earthquake, Pages 47-63.

Webster F, Tolles L (2000) Earthquake damage to historic and older adobe buildings during the 1994 Northridge, California Earthquake. Proceedings of 12th world conference on earthquake engineering, Auckland, New Zealand.

739 Zegarra L, Quiun D, San Bartolomé A, Giesecke A (1997) Reinforcement of Existing Adobe Dwellings
740 2nd part: Seismic Test of Modules. In Spanish. XI National Congress of civil Engineer. Trujillo,
741 Peru.

742 Zegarra L, Quiun D, San Bartolome A, Giesecke A (2001) Behavior of Reinforced Adobe Houses in
743 Moquegua, Tacna and Arica during the June 23, 2001 Earthquake (in Spanish). XIII National
744 Congress on Civil Engineering. Puno, Peru.